

Supplementary Information for:

Electromechanical coupling in elastomers: correlation between electrostatic potential and fatigue failure

Yan A. Santos da Campo,^a Dylan Mehler,^b Ezequiel Lorenzetti,^b Kelly S. Moreira,^b Ana L. Devens,^b Leandra P. dos Santos,^c Fernando Galembek,^c and Thiago A. L. Burgo^{*a,b}

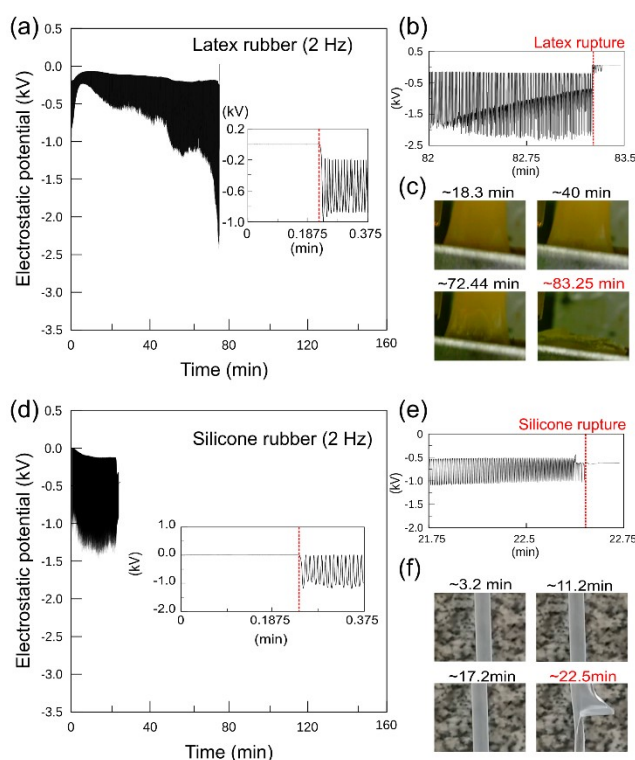


Fig. S1. Representative plots of the electrostatic potential of (a) natural rubber and (d) silicone rubber under stretching-relaxation cycles. The insets in (a) and (d) shows the zoom in at the beginning while (b) and (e) are the zoomed in plots close to the rupture of latex and silicone, respectively. Optical images for (c) latex and (f) silicone during the course of the experiment are shown along with the respective electrostatic potentials.

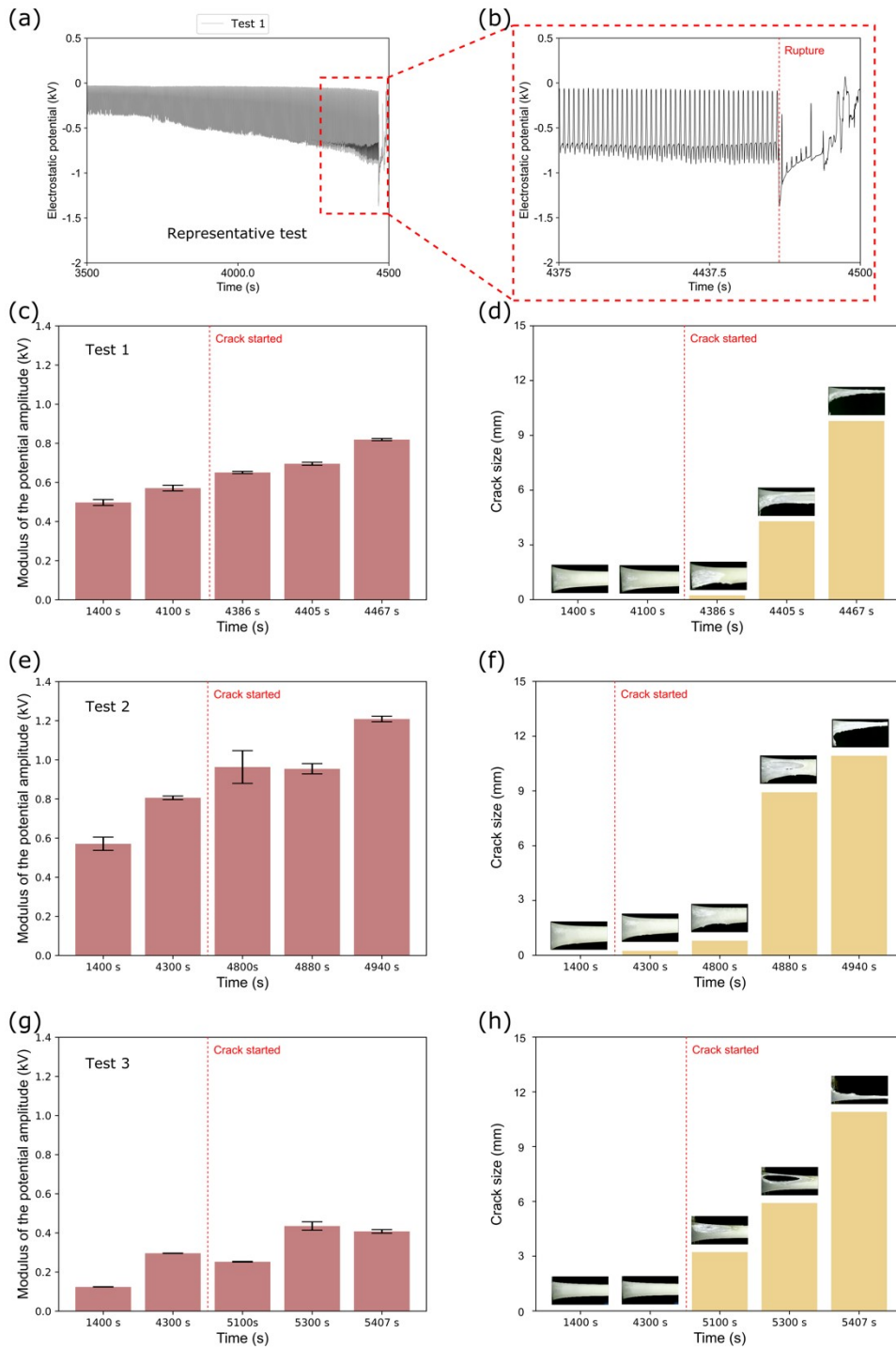


Fig. S2. (a) Representative plot of the electrostatic potential of natural rubber and (b) the zoom close to crack initiation. (c,e,g) Electrostatic potential amplitudes calculated at different moments were calculated using a total of 15 points (± 7 cycles for the selected period). The correspondent crack sizes presented along with the optical images for each period are shown in (d,f,h).

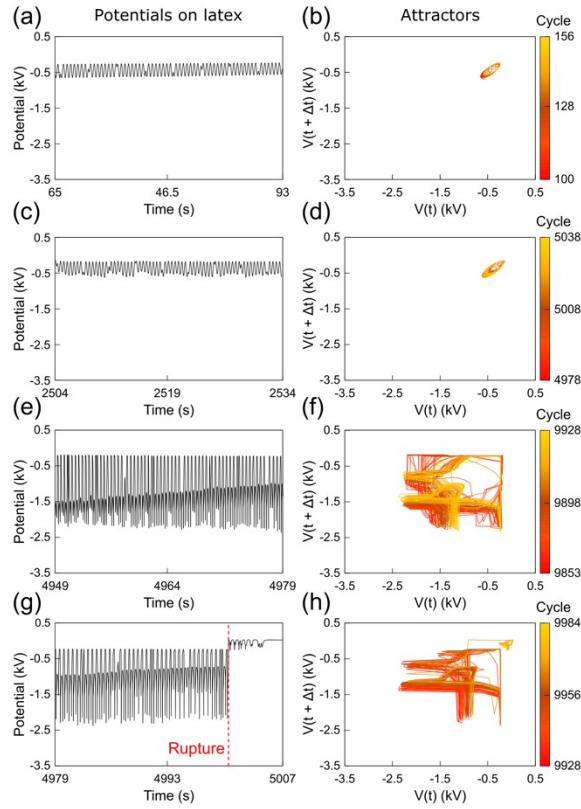


Fig. S3. (a,c,e,f) Sections of the recorded time-series of the electrostatic potential of periodically stretched natural latex and (b,d,f,h) the respective attractors. Periodic stretching-relaxation tests were performed at 2 Hz.

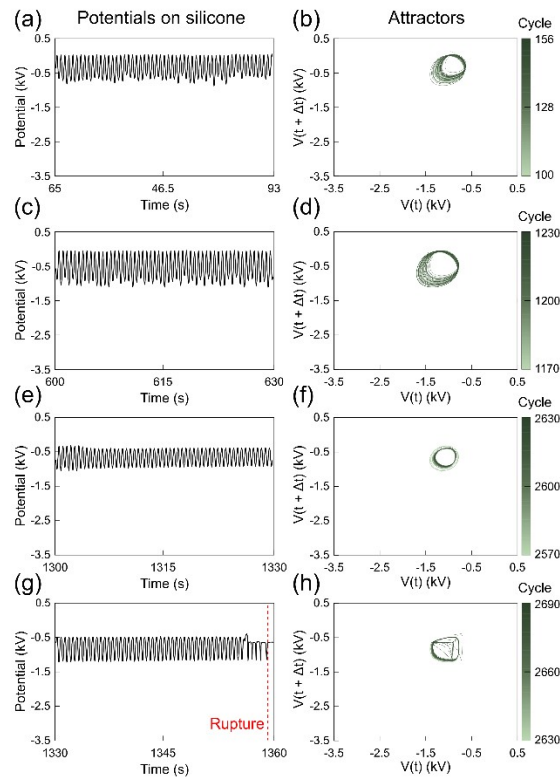


Fig. S4. (a,c,e,f) Sections of the recorded time-series of the electrostatic potential of periodically stretched silicone rubber and (b,d,f,h) the respective attractors. Periodic stretching-relaxation tests were performed at 2 Hz.

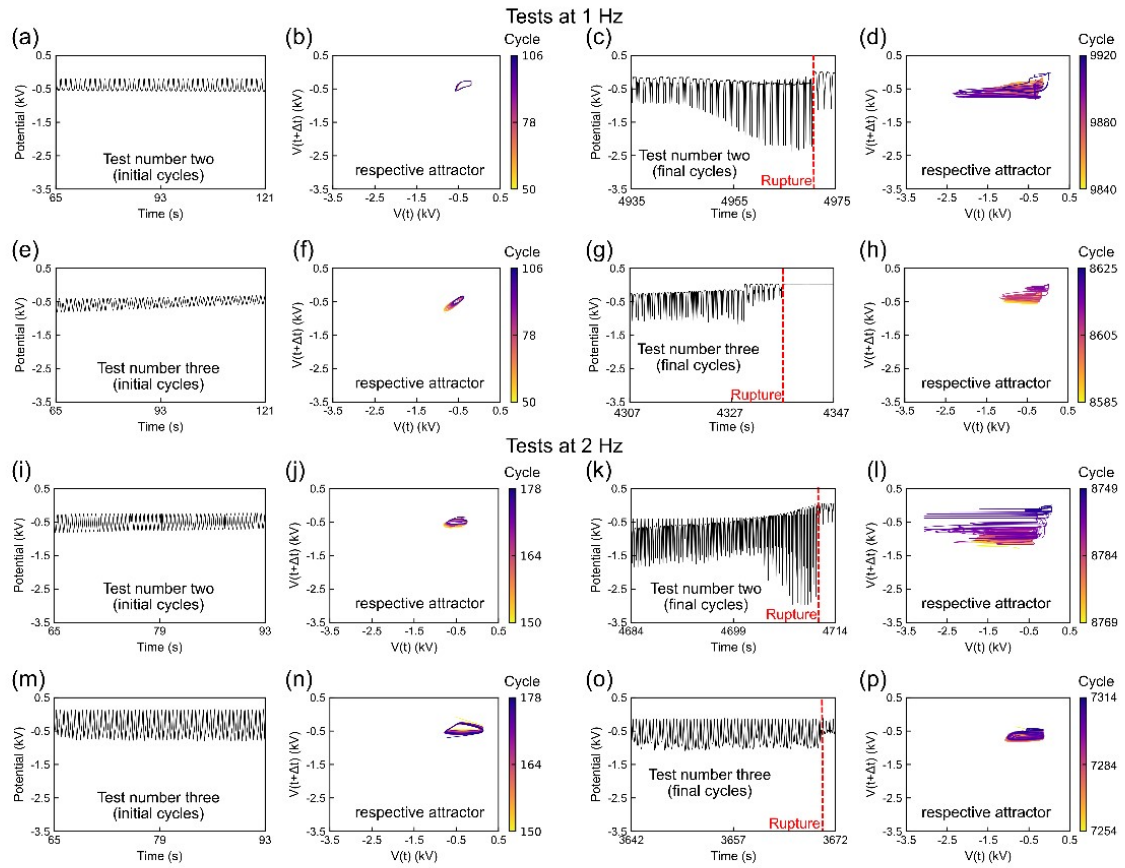


Fig.S5. Additional runs on the electrostatic potentials of natural latex under periodic stretching of 1Hz and 2 Hz presented with their respective attractors.

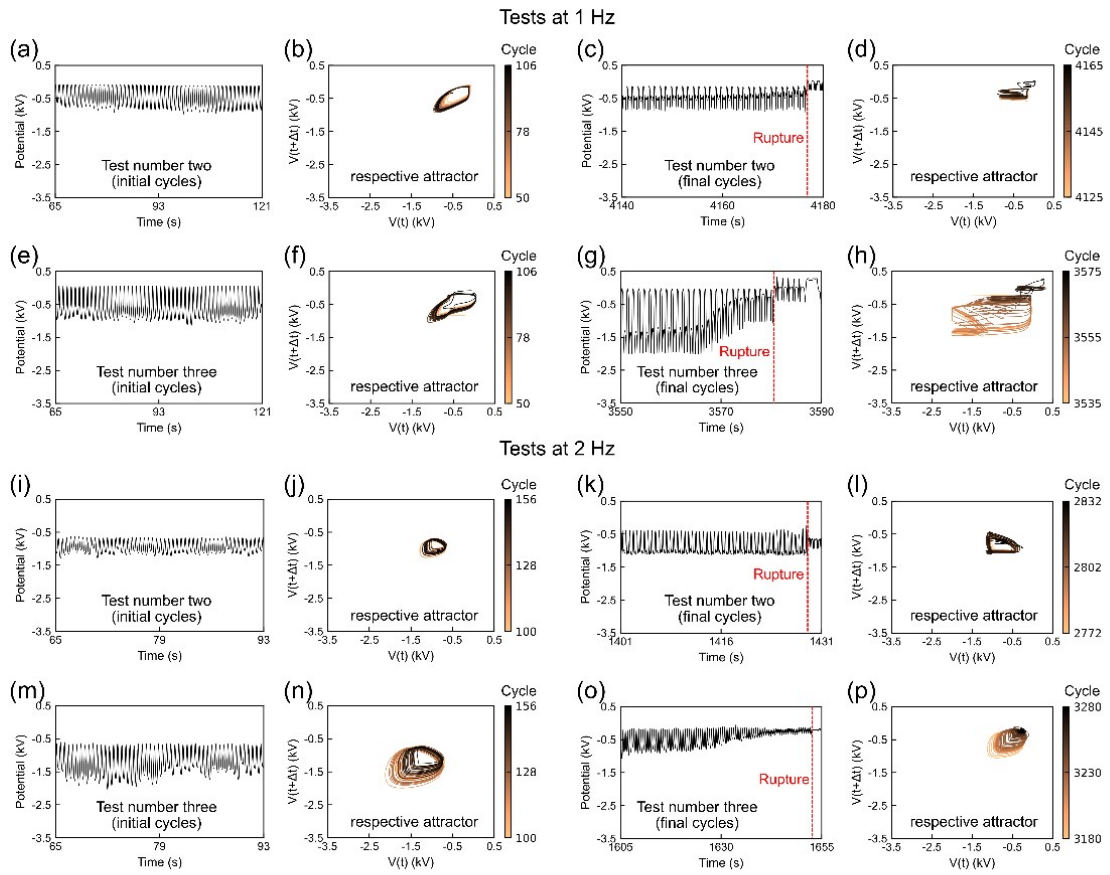


Fig.S6. Additional runs on the electrostatic potentials of silicone rubber under periodic stretching of 1 Hz and 2 Hz presented with their respective attractors.

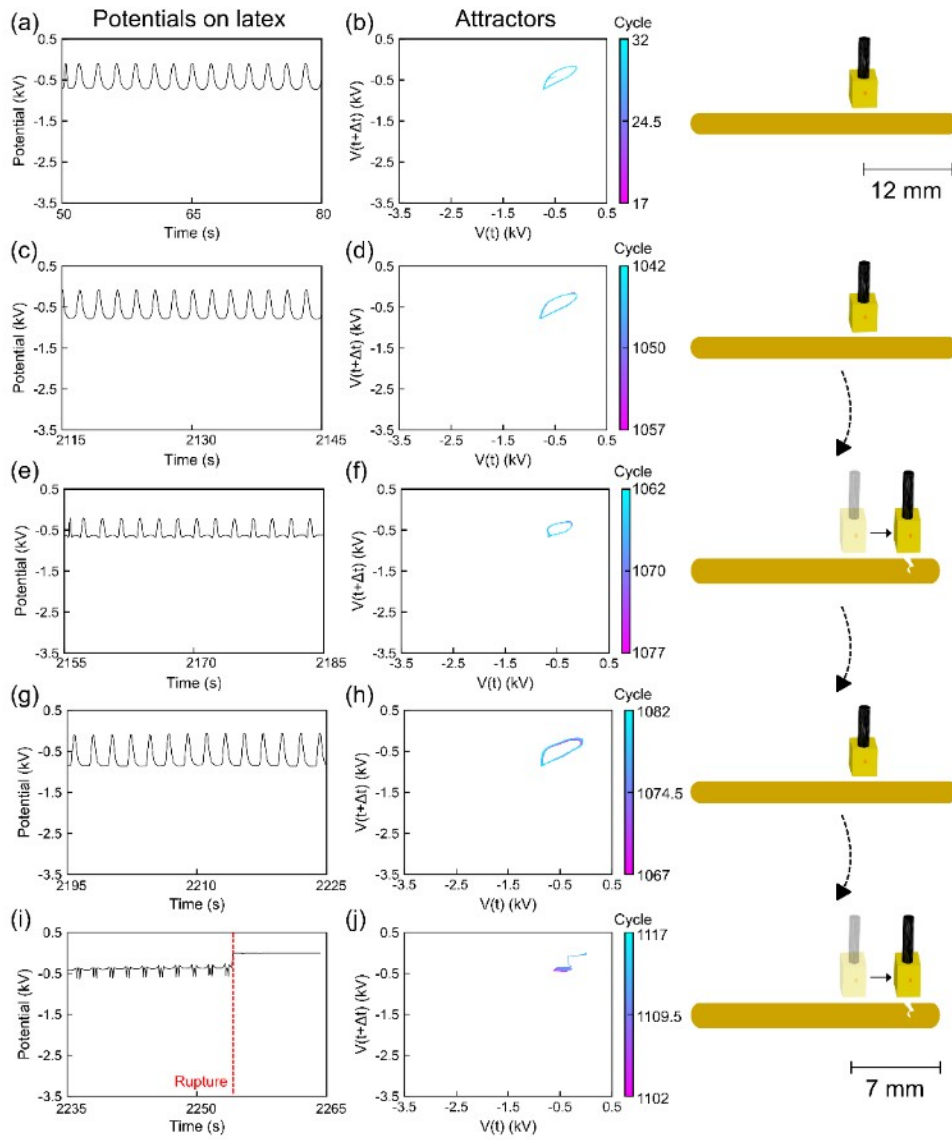


Fig.S7. (a) Electrostatic potential in the initial position in latex rubber tests at 0.5 Hz, (c, g) electrostatic potentials in the position outside the rupture region, (e, i) electrostatic potentials in the rupture region and (b, d, f, h, j) their respective attractors.

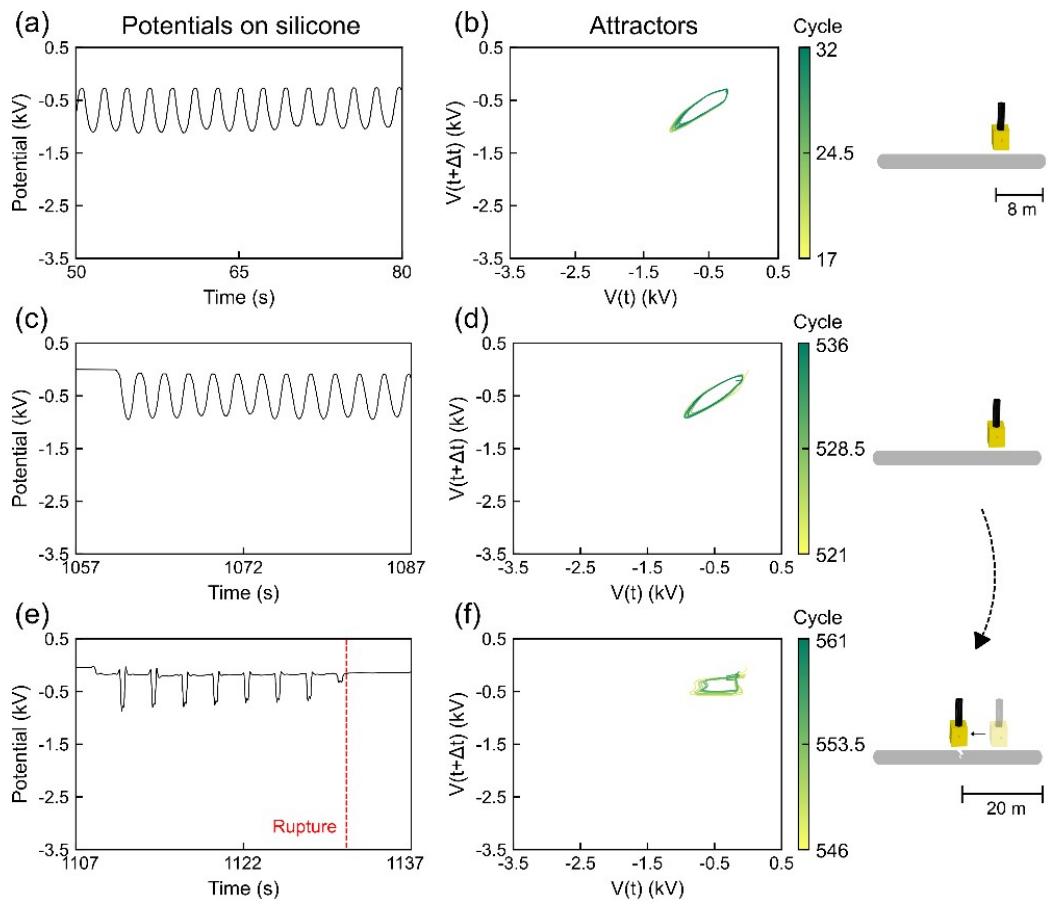


Fig.S8. (a) Electrostatic potential in the initial position in tests with silicone rubber at 0.5 Hz, (c) electrostatic potential in the position outside the rupture region, (e) electrostatic potential in the rupture region and (b, d, f) their respective attractors.

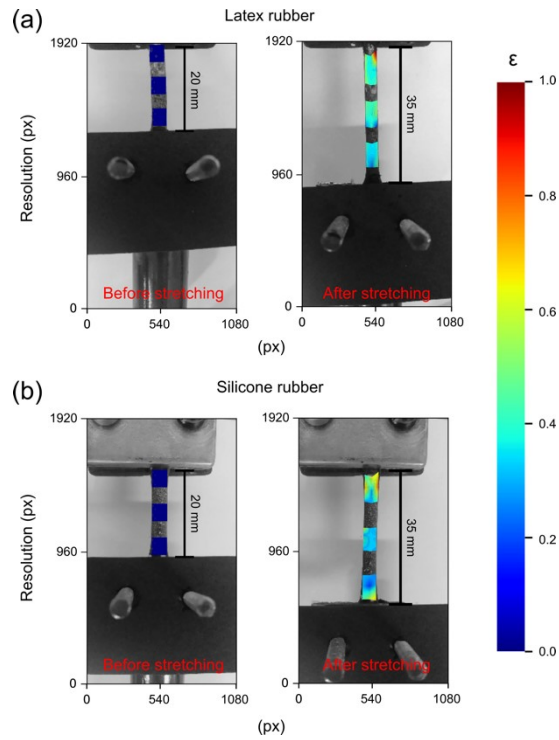


Fig. S9. Digital image correlation (DIC) of natural latex and silicone rubber. DIC was used to estimate the strain gradient of samples using in the stretching experiments. A python code was created using the DIC toolkit package¹. Samples were video recorded during the stretching process to 35 mm, using a cell phone camera with a resolution of 1920x1080 pixels. In the same python program, a routine was created to extract 30 frames per second from the video. The strain gradient was given in true strain (ϵ). By definition, the mechanical strain is given by $\epsilon = \Delta x/x$, where x is the position vectors in the initial configurations. Thus, $\epsilon_{true} = \ln(x_n/x_{n-1})$. This strain represents the current n strain tensor of the system, always in relation to the immediately preceding ($n-1$) strain tensor. Finite element method (FEM) is used for the numerical solution of the strain gradient.

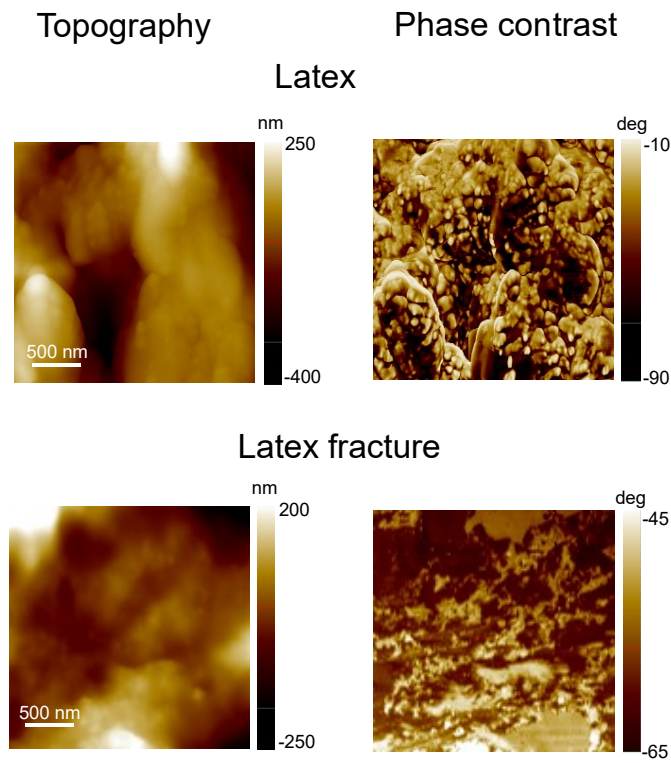


Fig. S10. AFM images of pristine latex (top) and the tested specimen (bottom).

References

¹ S. N. Olufsen, M. E. Andersen and E. Fagerholt, μ DIC: An open-source toolkit for digital image correlation, *SoftwareX*, 2020, **11**, 100391.